New Insights into the Use of (TD-)DFT for Geometries and Electronic Structures of Constrained π-Stacked Systems: [*n.n*]Paracyclophanes

Petrina R. N. Kamya and Heidi M. Muchall*

Centre for Research in Molecular Modeling and Department of Chemistry and Biochemistry, Concordia University, Montréal, Québec H4B 1R6, Canada

Received: September 12, 2008; Revised Manuscript Received: October 23, 2008

We have evaluated the performance of three (TD-)DFT functionals with the 6-31+G(d,p) basis set for the reproduction of experimental geometries, vertical ionization potentials, and low excitation energies of a selection of [2.2] and [3.3]paracyclophanes. Overall, (TD-)BH&H outperforms both (TD-)B3LYP and (TD-)PBE0. Some shortcomings are shown by B3LYP for geometries and by BH&H for ionization potentials. Most notably, whereas TD-B3LYP and TD-PBE0 reproduce the wavelength for the first electronic excitation of [*n.n*]paracyclophanes with weakly interacting aromatic rings, neither handles the strong donor−acceptor interactions in certain substituted [*n.n*]paracyclophanes, and both seriously underestimate the energy for their first electronic excitation. As the former systems are in many ways similar to stacked nucleic acid bases, we recommend the use of (TD-)PBE0/6-31+G(d,p) for further studies on π-stacking interactions in *constrained* systems, such as the base pairs in oligonucleotides.

1. Introduction

Despite the fact that weak dispersion-type interactions, such as those found in π-stacking, are known to be inadequately represented by most conventional density functional theory (DFT) methods when compared to higher correlated methods, the success of DFT methods in the reproduction of these very interactions in certain contexts is still reported.[1−8] However, although tremendous efforts have been made toward establishing which computational methods work best for dispersion-type interactions, most of the studies used to illustrate the shortcomings of DFT methods have been conducted on unconstrained, fully optimized, "stacked" benzene rings,[9−12] benzene derivatives,[9−12] and nucleic acid bases.[9,11,13−17] In most (if not all) of these studies, it has been reported that DFT methods fail to locate the stacked minimum-energy structures on the potential energy surfaces of these systems. This problem has been attributed in part to the asymptotic behavior of the exchange-correlation functionals that results in very weak or nonexistent contributions to the correlation energy, which incidentally also affects the proper description of long-range charge-transfer interactions in large aromatic biological molecules.[3,18] Other reasons for this failure have been attributed to the incomplete knowledge of the exact exchange-correlation functional[19] and the inability of DFT methods to account for static correlation.[20] The term unconstrained is used above to differentiate between these cases where aromatic rings are free to adjust the inter-ring distance and those where the rings are tethered or constrained. If DFT methods fail to reproduce the stacking in unconstrained π systems, the problems might be alleviated in tethered systems, for which [*n.n*]paracyclophanes are the perfect models.

Since the first reported synthesis of [2.2]paracyclophane (**1**, Chart 1),[21] [*n.n*]paracyclophanes have provided key insights into the effects of bringing two conformationally constrained benzene rings into close proximity. As a consequence of the short bridges between the aromatic rings in [2.2]paracyclophane, repulsive as opposed to stabilizing interactions occur between the π clouds in the inter-ring region that force the π density to the exterior faces of the aromatic rings, causing a boatlike deformation. The aromatic rings are twisted relative to one another, which partially relieves the torsion strain but, in turn, introduces additional strains that include a decrease of the inter-ring distance (IRD) and an elongation of the central C−C bridge bonds.[22,23] Increasing the length of the bridges by one carbon as in

CHART 1: [2.2]Paracyclophanes

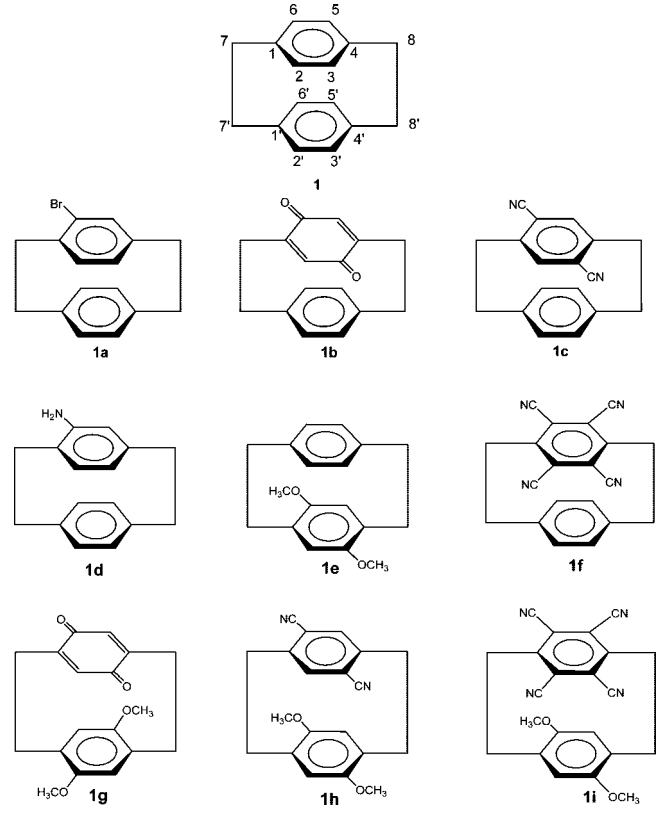

* To whom correspondence should be addressed. E-mail: muchall@alcor.concordia.ca. Phone: (514) 848-2424ext 3342. Fax: (514) 848-2868.

10.1021/jp808144e CCC: $40.75
Published on Web 12/04/2008

CHART 2: [3.3]Paracyclophanes

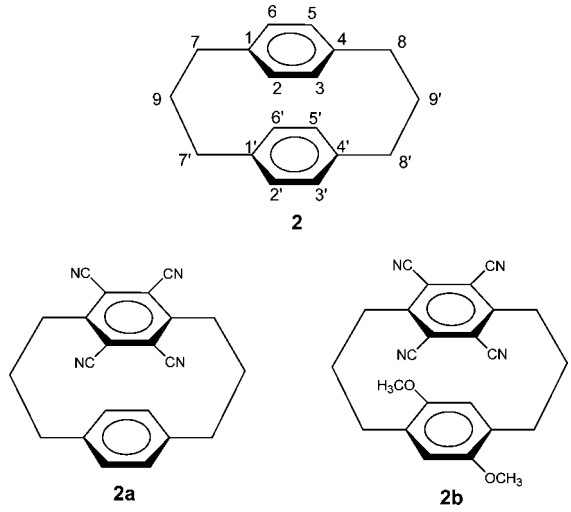

[3.3]paracyclophane (**2**, Chart 2) releases most of the steric strain in the molecule, providing enough space in the inter-ring region for stablizing π-stacking interactions.[24]

The interplay between steric strain and the distribution of π clouds in [*n.n*]paracyclophanes generates unique chemical environments that have been exploited in numerous organic and inorganic applications including studies involving cation$-\pi$ interactions[25] and selective catalysis.[26,27] [*n.n*]Paracyclophanes have also served as building blocks for various supramolecular compounds and polymers.[28,29] Recently, [2.2]paracyclophane has been used as a model system in computational studies to evaluate various model chemistries on their ability to reproduce the geometry of the global minimum.[1−3,6] Because the geometry is a function of the dispersive inter-ring interactions, an accurate reproduction of the geometry of **1** requires a good handle on electron correlation on the part of the method used. From these studies, it has been suggested that some DFT methods such as B3PW91 and PBE might, in fact, be able to handle long-range dispersion interactions well enough to capture their contribution to the overall geometry of **1**.[1−3]

Our interest in [*n.n*]paracyclophanes lies in their use as models for stacked oligonucleotide bases. In small [*n.n*]paracyclophanes, the tether between the interacting aromatic rings restricts their vertical displacement to distances ranging from approximately 2.7 to 3.4 Å, thus assuming a role similar to that of the sugar−phosphate backbone in oligonucleotides. Our ultimate aim is to select a DFT-based model chemistry that is able to characterize the H-bonding and π-stacking interactions in nucleic acid base pair subunits obtained from experimental structures of oligonucleotides. Our rationale for this investigation is simply that, if the electronic structure, with ionization potentials and excitation energies as observables, of [*n.n*]paracyclophanes can be reproduced, the model chemistry used to produce these results is adequate for our intended purposes.

The present article is an investigation of selected DFT methods and one correlated method in terms of their abilities to reproduce the geometries, ionization potentials, and excitation energies of various [*n.n*]paracyclophanes. The compounds were selected to reflect a range of geometries and interactions between the two aromatic rings. Chart 1 shows [2.2]paracyclophane (**1**) and its derivatives with substitution on one ring (**1a**−**1f**) and on both rings (**1g**−**1i**). Chart 2 shows [3.3]paracyclophane (**2**) and its derivatives (**2a** and **2b**).

2. Computational Methods

All calculations were performed using the Gaussian 03 suite of programs.[30] Two common hybrid DFT methods,[31] Becke's three parameter hybrid exchange functional[32] with Lee, Yang, and Parr's correlation functional,[33] denoted B3LYP,[34] and the parameter-free Perdew−Burke−Ernzerhof[35] (PBE0) functional were employed. Both functionals are known to be a good compromise between computational cost and the accuracy of results obtained, compared to higher correlated methods, and have been shown to be capable of quantifying H-bonding interactions between nucleic acid bases, which is important for our future studies.[36,37] The time-dependent PBE0 method has also recently been shown to reproduce the lowest-energy singly excited state of the stacked cytosine dimer with an accuracy comparable to that of CASPT2.[38] In addition, these DFT methods have been chosen because of the controversy surrounding their abilities to capture dispersion-type interactions.[3,11]

Becke's half-and-half functional (BH&H) as it is implemented in Gaussian 03 was employed because of its reported ability to adequately characterize dispersion interactions.[39] It is a hybrid half-and-half functional, where the exchange-correlation energy is calculated from Hartree−Fock (HF) and local spin-density approximation (LSDA) exchange and LYP correlation energies as

$$E_{XC} = 0.5E_X^{HF} + 0.5E_X^{LSDA} + E_C^{LYP} \quad (1)$$

For comparison, a correlated ab initio quantum chemical method, second-order Møller−Plesset (MP2),[40] was included, as it is generally considered better suited for the calculation of dispersion-type interactions despite the fact that it is known to overestimate these types of interactions.[17,41] The particular combination of MP2 with a medium-sized basis set has also previously been reported as being ideal for the reproduction of the geometry of [2.2]paracyclophane.[2,6]

Geometry optimizations and frequency calculations were carried out using Pople's double or triple split-valence basis sets with diffuse and polarization functions.[42] All optimized geometries are minima on their potential energy surfaces as indicated by the absence of imaginary frequencies. Bearing in mind that our aim is to identify a usable, medium-sized basis set, we evaluated the performances of the 6-31G, 6-31+G(d,p), and 6-311+G(d,p) basis sets with B3LYP and PBE0 functionals in reproducing the ionization events of substituted and unsubstituted [2.2]paracyclophanes. As there was a significant improvement when diffuse and polarization functions were included compared to when the basis set increased from double- to triple-ζ (Figure S1 in the Supporting Information), all analyses presented in this article were performed with the 6-31+G(d,p) basis set.

First vertical ionization potentials ($IP_{v,1}$) were calculated as the difference in total energies between a molecule and its radical cation, at the geometry of the former. Higher ionization energies ($IP_{v,1+n}$) were calculated from the orbital energies (ε) by applying Koopmans' theorem ($IP_v \approx -\varepsilon$).[43] According to eqs 2 and 3, the energy difference between $IP_{v,1}$ and the HOMO energy is added to the energies of the next higher orbitals (ε_{HOMO-n}) as a uniform shift.[44] All total and zero-point vibrational energies are listed in Tables S1−S7 of the Supporting Information.

$$IP_{v,1} - (-\varepsilon_{HOMO}) = \Delta E \quad (2)$$

$$-\varepsilon_{HOMO-n} + \Delta E = IP_{v,1+n} \quad (3)$$

When dealing with large molecules, time-dependent density functional theory (TD-DFT) is often the method of choice for

the calculation of excited states, as it has been shown to be reliable for aromatic systems such as substituted phenols,[45] *o*-chloranil/aniline complexes,[38,46] and the cytosine dimer,[38] even though the use of TD-DFT for electronic transitions with significant charge-transfer (CT) character has been questioned.[47−49] We have used TD-B3LYP, TD-PBE0, and TD-BH&H to calculate the first few excitation energies. The UV−vis spectra were simulated using the SWizard program, revision 4.4, with the Gaussian model.[50] The band half-widths were taken to be equal to 3500 cm^{-1}. Molecular orbitals were plotted using Molekel 4.3.[51]

3. Results and Discussion

3.1. Geometries. ***3.1.1. [2.2]Paracyclophanes.*** The correct representation of the geometry of [2.2]paracyclophane (**1**) with respect to its point group has been shrouded in controversy for many years.[1−3,6,7,9,22,23] The most recent publication that addresses the issue indicates that the minimum-energy geometry of **1** obtained with MP2/6-31+G(d,p) is of D_2 symmetry, reduced from D_{2h} symmetry by torsion strain in accord with the dynamic disorder found in the crystal at room temperature.[1,23]

Table S8 of the Supporting Information lists the geometrical parameters of **1** from full geometry optimizations using B3LYP/6-31+G(d,p), BH&H/6-31+G(d,p), and PBE0/6-31+G(d,p); those from MP2/6-31+G(d,p) reported earlier;[2] and the X-ray crystal data determined experimentally.[23] The geometrical parameters and the atom numbering in Table S8 were chosen based on those selected by Caramori et al.[2] In general, the DFT methods perform with an accuracy close to that of MP2, with one notable exception. Although B3LYP/6-31+G(d,p) reproduces the bond lengths and angles rather well, it predicts a geometry with close-to-D_{2h} symmetry and therefore fails to reproduce the most important property, that is, the degree of twist in the methylene bridge, which is defined by the dihedral angle C1−C1′−C7−C7′ (see atom numbering in Chart 1 and value for torsion angle in Table 1). This underestimated torsion angle from B3LYP/6-31+G(d,p) was discussed previously, and it was suggested that an inadequate representation of the torsional strain for the eclipsed bridges might be the cause.[2] In contrast, with the PBE0 and BH&H functionals, not only is the twist reproduced, but the calculated torsion angle deviates from the reported experimental value even less than that from MP2. From Table 1, BH&H shows the closest agreement with experiment for this parameter; the PBE0 value is closer to experiment if compared to the more recently reported torsion angle of 12.6° from X-ray crystal data at 19 K.[3] Finally, both PBE0 and BH&H exhibit superior performance to B3PW91 (reported earlier).[2]

The addition of donor or acceptor groups to the aromatic rings in **1** relieves the degree of strain by modifying the π-density distribution, which generates changes to the overall geometry.[52,53] Because of the availability of their crystal structures, only **1f**, **1h**, and **1i** (Chart 1) are included here. Because BH&H and PBE0 performed as well as MP2 in reproducing the geometry of **1**, the more expensive MP2 was not included in this evaluation. Tables S9−S11 in the Supporting Information, with the geometrical parameters and the atom numbering taken from Staab et al.,[52] contain the full sets of geometries for **1f**, **1h**, and **1i**. Table 1 compiles three important geometrical parameters for **1**, **1f**, **1h**, and **1i**. These are the degree of twist between the parallel aromatic rings, the inter-ring distance (IRD) taken between C1 and C1′ or C4 and C4′, and the boatlike deformation of the aromatic rings. For ease of comparison, the atom numbers in Table 1 for the substituted [2.2]paracyclophanes are as given for **1** in Chart 1. The experimental trend in the twist is a general reduction upon substitution, with nonzero dihedral angles for all compounds. Again, B3LYP underestimates the degree of twist and therefore determines the wrong point group for **1f**, as it did for **1**, even though full symmetry is not achieved. All methods overestimate the degree of twist in **1i** (Table 1). This might be a consequence of the reported intermolecular stacking found in the crystal structure for **1i**,[52] which is absent in the gas-phase calculations, a situation similar to that found in crystal and gas-phase geometries of biphenyls.[54−56]

TABLE 1: Selected Experimental and Calculated [6-31+G(d,p) Basis Set] Geometrical Parameters for 1, 1f, 1h, and 1i

	exptl[a]	B3LYP	PBE0	BH&H	MP2[b]
		Degree of Twist[c]			
1	16.1	1.2	11.5	17.8	22.2
1f	11.5, 9.4	0.0	4.4	14.6	
1h	15.8	17.7	19.6	23.1	
1i	8.7[d]	16.8	17.2	19.9	
		Inter-Ring Distance[e]			
1	278.2	283.1	279.8	275.9	277.1
1f	274.4	280.3	276.5	272.5	
1h	273.0[d]	282.0	278.1	273.6	
1i	274.0	280.4	276.2	271.8	
		Degree of Boatlike Deformation[f]			
1	153	152	152	152	152
1f	154, 151	153	153	153	
1h	153	152	152	152[d]	
1i	154[d]	152	153[d]	153[d]	
		Out-of-Plane Twist of Methoxyl Groups[g]			
1h	9.6[d]	11.5	11.1	13.6	
1i	8.0, 5.2	13.2	12.0	13.3	

[a] X-ray data from ref 23 (**1**), ref 52 (**1f** and **1i**), and ref 53 (**1h**). [b] From ref 2. [c] Given by the torsion angles C1−C7−C7′−C1′ and C4−C8−C8′−C4′ in degrees (identical if one value is listed). [d] Average value for a difference in distances of 0.3 pm and in angles of 1° or less. [e] Given by the distances C1−C1′ and C4−C4′ in pm (identical if one value is listed). [f] Average bend for each ring given by the torsion angles C2−C3−C4−C8, C3−C2−C1−C7, C6−C5−C1−C7, and C5−C6−C1−C7 and corresponding torsion angles for the second ring in degrees (identical if one value is listed). [g] Given by the torsion angles C2′−C3′−O−CH_3 and C5′−C6′−O−CH_3 in degrees (identical if one value is listed).

The experimental inter-ring distance (IRD) between the bridgehead carbon atoms is reported to be smaller in the substituted compounds compared to **1**,[52] with the smallest IRD in **1h**.[53] The decrease in IRD that accompanies the introduction of donor and acceptor groups demonstrates an increase in favorable charge-transfer interactions[53] and a decrease in the amount of repulsion between the aromatic rings.[52] All methods reproduce the experimental trend of decreased IRDs relative to **1** (Table 1). In general for all molecules considered, B3LYP overestimates the IRDs, possibly because of inadequate treatment of dispersion interactions between the two aromatic rings, as has been reported with the unconstrained stacked systems in the literature.[3,4,11,17] Finally, that there is hardly any difference in the experimental IRD when directly comparing **1f** and **1i**, even though the stronger electron-donating groups in **1i** result in a longer-wavelength electronic transition compared to **1f**,[52] was ascribed to the rigidity of [2.2]paracyclophanes, which does not permit drastic changes to the geometry due to electronic effects.[52] In this respect, it is remarkable that PBE0 and particularly BH&H indeed determine smaller IRDs for **1i**.

We chose to represent the boatlike deformation of the aromatic rings through the C2−C3−C4−C8 torsion angle and

CHART 3: Conformers of 2

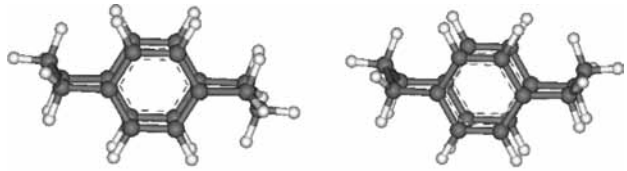

its counterparts, where 180° indicates planarity. All methods reproduce the experimentally reported substantial boatlike deformation in all systems with high accuracy (Table 1). The increased nonplanarity reported for the tetracyano-substituted ring in **1f**, on the other hand, is not captured by the calculations. This discrepancy might again be due to the intermolecular packing of the molecules in the crystal, favoring a more bent aromatic acceptor ring that would facilitate the stacking.

With respect to the methoxyl substituents in **1h** and **1i**, one other finding is worth reporting. An analysis of the X-ray geometry of **1h**[53] shows that the methoxyl groups deviate from the sp^2 "plane" of the aromatic ring to a larger degree than those in **1i**.[52] A similar out-of-plane twist has been reported in the X-ray structure of 1,2-dimethoxybenzene.[57] All methods overestimate this out-of-plane twist of the methoxyl substituents of **1h** and**1i**, with larger differences for **1i** (Table 1). This is once again probably due to changes between the gas phase, where the molecules are not stacked, and the crystal, where **1i** shows a higher degree of stacking than **1h**, causing the methoxyl groups to adopt a more in-plane conformation.

3.1.2. [3.3]Paracyclophanes. The longer bridges between the aromatic rings in [3.3]paracyclophanes provide these molecules with more flexibility than their [2.2]paracyclophane counterparts, thus allowing the effects of substitution on the overall geometry to be more apparent and increasing the variability of the test set of compounds.[52] Gantzel and Trueblood showed that the crystal structure of [3.3]paracyclophane (**2**) has somewhat deformed aromatic rings that exhibit a bent-boat conformation, with a slight twist of one ring relative to the other.[58] The trimethylene groups of the tethers are in a conformation that is similar to that in gauche *n*-butane, and they adopt an anti conformation with respect to each other that is now more widely referred to as chair (Chart 3).[58] Anet and Brown showed that **2** actually adopts two conformations in solution, the chair and the boat (syn conformation, Chart 3).[59] The relative ratio of chair to boat in $CDCl_3$—$CDCl_2F$ solution at −88 °C was determined to be about 1:2.[59] Similarly, **2b** has been determined to exist as 40% chair and 60% boat in the crystal.[52] Gas-phase calculations on the relative ratio of chair to boat conformers have not been conducted (to the best of our knowledge), the assumption being that the distribution should be similar to that in solution.[60] We have performed geometry optimizations on [3.3]paracyclophane (**2**) and its derivatives (**2a** and **2b**) using B3LYP, PBE0, and BH&H functionals with the 6-31+G(d,p) basis set. Population distributions for each compound were calculated from zero-point corrected energies at 185 or 298 K, and as with the [2.2]paracyclophane series, we have compared the calculated geometries to experimental data.[52]

Table 2 shows the experimental and calculated population distributions for **2**, **2a** and **2b**. For **2**, the population of conformers in solution is close to that found in the gas phase with B3LYP and PBE0; BH&H on the other hand predicts a 50:50 distribution. Because of the facts that we are attempting to reproduce solution NMR results in the gas phase, and that the energy difference between the two conformers is small (ΔE < 0.8 kcal mol^{-1}), it is safe to state that all methods perform well. While there are no experimental data on the population distribution of **2a**, all methods agree on a large preference for the boat. For **2b**, only BH&H reproduces the experimental preference for the boat, but again, the energy differences determined with all methods are small, and distributions in the crystal and the gas phase are not necessarily comparable.

TABLE 2: Experimental and Calculated[a] [6-31+G(d,p) Basis Set] Population Distributions (%) of 2, 2a, and 2b

	exptl	B3LYP	PBE0	BH&H
2 chair	33[b]	39 (32)[c]	40 (35)[c]	50 (51)[c]
2 boat	66[b]	61 (68)[c]	60 (65)[c]	50 (49)[c]
2a chair		31	13	14
2a boat		69	87	86
2b chair	40[d]	70	67	48
2b boat	60[d]	29	33	52

[a] With zero-point vibrational energy corrections at 298 K. [b] Given as chair/boat = 1:2 in ref 59. [c] With zero-point vibrational energy corrections at 185 K. [d] From ref 52.

Tables S12−S14 in the Supporting Information show the experimental and calculated geometric parameters of **2**, **2a**, and **2b**. The important geometrical parameters are compiled in Table 3. We are once again interested in those parameters that best reflect the electronic structure of the molecules, namely, the degree of twist, the IRD, and the degree of boatlike deformation of the aromatic rings.

All methods capture the overall release in strain brought about by the longer tether in **2** compared to **1**. The degree of twist between the aromatic rings is smaller, the IRDs are longer, and the degree of boatlike bend of the aromatic rings is significantly less (Table 3). However, even though the experimental value is small, both B3LYP and PBE0 fail to predict a nonzero value for the degree of twist in **2**, whereas BH&H succeeds in this prediction. The experimental trend in the IRD shows that, as for the [2.2]paracyclophanes, upon substitution, the IRD decreases, and this trend is reproduced by all methods. However, the calculated IRDs for **2** and **2b** show that B3LYP overestimates the distance on average by approximately 10 pm, demonstrating once again that this method underestimates the extent of interaction between the two rings. PBE0 and BH&H predict IRDs that are closer to experiment (Table 3). Compared to **1**, the aromatic rings in **2** are significantly less bent, with values closer to 180°.[58] All functionals reproduce the degree of boatlike deformation with differences from the experimental values of 1° or less (Table 3).

As in **1i**, the methoxyl substituents in **2b** are not "coplanar" with the aromatic ring (Table 3).[52] Whereas B3LYP predicts identical values for the chair and boat, for PBE0, the C—C—O—C twist is less in the boat conformer, and for BH&H, this twist is less in the chair conformer. There is thus a correlation between the C—C—O—C twist and the stability of the conformers, in line with the fact that, for methoxybenzenes (anisoles), the methoxyl group generally lies in the plane of the aromatic ring.[45,55]

3.2. Ionization Energies. The proximity of the two conformationally constrained aromatic rings in [*n.n*]paracyclophanes is known to influence the electronic structure of these molecules in a way that is reflected in their photophysical behavior.[60] As there is a large collection of photoelectron (PE) spectra of [*n.n*]paracyclophanes in the literature, a reproduction of the ionization energies of these molecules can be used as a means of further evaluating how well the selected functionals can reproduce their electronic structure. In this section, we compare

TABLE 3: Selected Experimental and Calculated [6-31+G(d,p) Basis Set] Geometrical Parameters for 2, 2a, and 2b

	exptl[a]		B3LYP		PBE0		BH&H	
	chair	boat	chair	boat	chair	boat	chair	boat
				Degree of Twist[b]				
2	5.0		0.0	0.0	0.0	0.0	7.3	1.6
2a			5.0	5.7, 3.7	6.2	3.3	7.9	4.0[c]
2b		7.1, 1.0	1.8	4.2, 0.5	1.8	6.4, 0.9	1.2	8.9, 0.2
				Inter-Ring Distance[d]				
2	313.7		323.9	324.5	319.0	319.4	310.9	312.8
2a			320.4[c]	320.6	314.9	315.1	306.9	307.3
2b		309.9, 306.8	319.6	320.3[c]	313.8	314.1[c]	304.9	304.9, 302.1
				Degree of Boatlike Deformation[e]				
2	168		167	167	168	168	168	168
2a			168	164, 168	169[c]	169[c]	170, 168	170, 169
2b		170[c]	168[c]	168	170[c]	169	170	171, 169
				Out-of-Plane Twist of Methoxyl Groups[f]				
2b		7.7, 5.8	7.6	7.6	5.5	5.7, 2.7	2.5	5.6, 7.0

[a] X-ray data from ref 58 (**2**) and ref 52 (**2b**). [b] Given by the improper torsion angles C1−C7−C7′−C1′ and C4−C8−C8′−C4′ in degrees (identical if one value is listed). [c] Average value for a difference in distances of 1 pm or less and in angles of 1° or less. [d] Given by the distances C1−C1′ and C4−C4′ in pm (identical if one value is listed). [e] Average bend for each ring given by the torsion angles C2−C3−C4−C8, C3−C2−C1−C7, C6−C5−C1−C7, and C5−C6−C1−C7 and corresponding torsion angles for the second ring in degrees (identical if one value is listed). [f] Given by the torsion angles C2′−C3′−O−CH_3 and C5′−C6′−O−CH_3 in degrees (identical if one value is listed).

ionization data from available published PE spectra to calculated IPs using B3LYP, PBE0, BH&H, and MP2 methods for **1** and B3LYP, PBE0, and BH&H for **1a**−**1e**, **1g**, **1h**, and **2**. This particular group of compounds was chosen for their wide range of ionization potentials that reflect the variety in their electronic structures and therefore pose a suitable challenge for the methods considered. All experimental vertical ionization potentials were taken from refs 60 and 61 and the original references therein. Tables S15−S17 of the Supporting Information contain the numerical IP data for all compounds considered.

Plots showing correlations between calculated and experimental values for the first five ionization events of **1** and **2** (boat conformer) are shown in Figure 1a,b, respectively. All methods reproduce the vertical ionization potentials of **1** and **2** rather well, with R^2 values in most cases close to 0.99. Yet only the B3LYP and PBE0 correlations exhibit slopes of close to 1.0 (1.03 and 1.05, respectively, for **1**; 1.04 and 1.06, respectively, for **2**), whereas those from BH&H (1.27 for **1**, 1.26 for **2**) and MP2 (1.67) are much steeper, resulting in a progressively more serious overestimation of the higher IPs. The B3LYP performance here is particularly encouraging, as it shows that, although it, in particular, did not perform as well as BH&H and PBE0 when reproducing the geometrical parameters of **1** and **2**, it does not fail to grasp the necessary electronic effects required to reproduce their PE spectra.

Substitution in [2.2]paracyclophanes leads to donor−acceptor interactions in the molecule that produce changes in the PE spectra that depend on the placement and nature of the functional groups.[61] Figure 2 shows the correlations between the calculated first five ionization events for **1a**−**1e**, **1g**, **1h**, and **2** and their experimental IPs. The compounds included in this analysis can be divided into two groups: those with orbital contributions from only one ring and those with orbital contributions from both rings. Chart 4 shows one example for each. Instinctively, one would expect the DFT methods to be successful in reproducing the low-energy ionizations of the former, given that, from an orbital perspective, these are simply aromatic compounds with para substitution. However, Figure 2 shows that all methods are able to reproduce the experimental IPs of all of the compounds, regardless of whether orbital coefficients are found

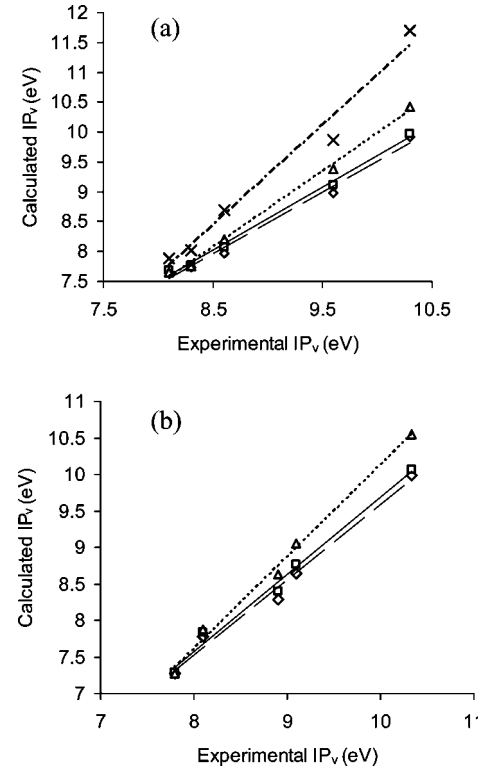

Figure 1. Correlations between the first five experimental and calculated vertical ionization potentials (eV) of (a) **1** and (b) **2** (boat conformer). Correlations are (a) (− − −) B3LYP (◇, $R^2 = 0.9876$), (—) PBE0 (□, $R^2 = 0.9950$), (• • •) BH&H (Δ, $R^2 = 0.9958$), (− • −) MP2 (×, $R^2 = 0.9744$) and (b) (− − −) B3LYP (◇, $R^2 = 0.9868$), (—) PBE0 (□, $R^2 = 0.9898$), (• • •) BH&H (Δ, $R^2 = 0.9934$).

on one or both rings, and that the $\pi-\pi$ interaction of the two rings in the latter case is adequately captured. Finally, we note that the BH&H data points exhibit a much more pronounced scatter than those for the other two functionals, and its correlation shows the above-mentioned deviation from a perfect slope (slopes are B3LYP, 0.99; PBE0, 1.02; BH&H, 1.23).

3.3. Excitation Energies. The substituted [2.2]paracyclophanes **1f** and **1i** and [3.3]paracyclophanes **2a** and **2b** (Charts

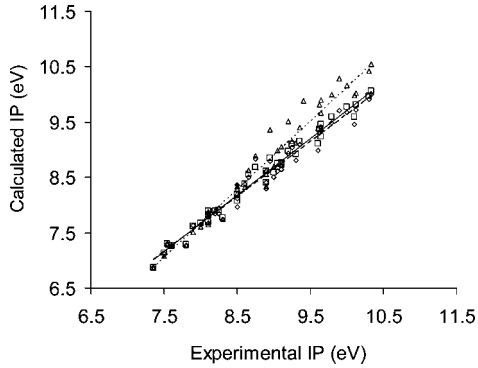

Figure 2. Correlations between experimental and calculated vertical ionization potentials for **1**, **1a**−**1e**, **1g**−**1h**, and **2**. (− − −) B3LYP (◇, $R^2 = 0.9691$), (—) PBE0 (□, $R^2 = 0.9841$), (• • •) BH&H (Δ, $R^2 = 0.9608$).

CHART 4: Highest Occupied Molecular Orbitals (HOMOs) of 1 and 1b

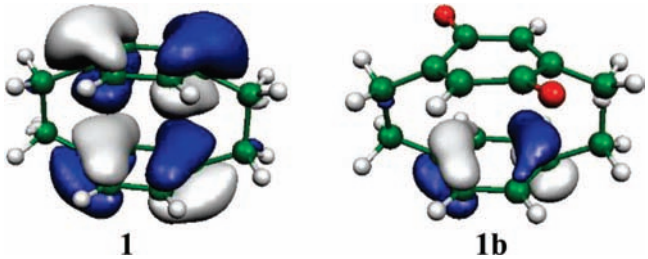

1 and 2) have a tetracyanobenzene ring as a common electron acceptor. The variety in this group of compounds stems from differences in the strengths of the donor rings and from the donor−acceptor ring distances. Staab et al. have shown that these two properties have an effect on the geometries and charge-transfer properties of the molecules.[52] Whereas we showed above that the effects of substitution on the geometries of **1f** and **1i**, in particular, are small, the effects on the charge-transfer properties of these molecules are so dramatic that they can be examined visibly with the naked eye.[52] Compound **1f**, with the weaker donor, is yellow; **1i**, with the stronger donor ring, is a deep violet. Keeping the dimethoxyl substitution and increasing the donor−acceptor distance from **1i** to **2b** results in a change in color from deep violet to dark red.[52] Quantitatively, these compounds exhibit "phane-specific" changes that are displayed in their UV−vis spectra (in chloroform) and consist of broadening of absorption bands, loss of vibronic structure, and the appearance of new absorptions. More specifically, whereas the charge-transfer transition in **1f** gives rise to a small shoulder at 395 nm, strengthening the donor (**1i**) results in a large bathochromic shift to 520 nm.[52] A larger distance between the rings results in a somewhat smaller red shift from 416 nm for **2a** to 508 nm for **2b** (a blue shift from **1i**). This shows that the longer donor−acceptor distance causes a similar but less pronounced effect on the charge-transfer transition compared to the substituted [2.2]paracyclophanes.[52]

We calculated the excitation energies of **1**, **1f**, **1i**, **2**, **2a**, and **2b** using time-dependent density functional theory (TD-DFT) and simulated the UV−vis spectra from the TD-DFT output. The parent compounds **1** and **2** are included in this part of the study as their UV−vis spectra are readily available and their longest-wavelength transitions are closest to those of stacked nucleic acid base pairs (240−260 nm).[62] An overlay of the experimental[24] and simulated spectra for **1** is shown in Figure 3. Selected simulations for **1**, **2** (boat conformer), and **2b** (chair

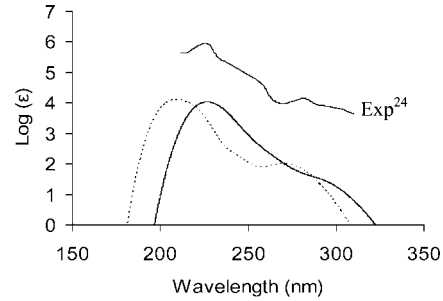

Figure 3. Overlay of experimental[24] and simulated [6-31+G(d,p) basis set; (—) TD-PBE0 and (• • •) TD-BH&H] UV−vis spectra of **1**.

conformer) are shown in Figure 4, with particular focus on the long-wavelength band for each (see insets). Numerical data for the lowest-energy transitions in **1**, **1f**, **1i**, **2**, **2a**, and **2b** can be found in Table 4.

Figure 3 shows the overall good agreement between the experimental spectrum and the spectra simulated from TD-PBE0 and TD-BH&H for **1**, the latter functional giving rise to a spectrum that shows more of the experimental features. The TD-B3LYP spectrum is similar to that from TD-PBE0, but because it is even more featureless than that from TD-PBE0, it is omitted for clarity. It is noted that the TD-BH&H spectrum is shifted to higher energies relative to that from TD-PBE0. With respect to the lowest-energy transition, the simulated UV spectrum for **1** (Figure 4a) obtained with TD-PBE0 or TD-BH&H shows good agreement with experimental data (λ_{max} of 302 nm, Table 4), in that a shoulder at about 290 nm or a distinct band at about 270 nm, respectively, can be seen (Figure 4a inset). In the spectrum from TD-B3LYP, on the other hand, even though an allowed transition at 271 nm is calculated (Table 4), this band is not discernible.

As for **1**, the simulated UV spectra of the boat conformer of **2** (Figure 4b) show that TD-BH&H produces a spectrum that is shifted to shorter wavelengths, resulting in too low a value for λ_{max} of the lowest-energy transition. In contrast, TD-B3LYP and TD-PBE0 predict the longest absorption wavelength close to the experimental value of 294 nm (Figure 4b inset). All methods, however, are in agreement insofar as only the boat conformer exhibits an allowed long-wavelength transition close to the reported literature value (Table 4). This difference in spectroscopic behavior of the two conformers is yet to be confirmed experimentally.

For the tetracyanobenzene series **1f**, **1i**, **2a**, and **2b** as a whole, it is obvious from Table 4 that neither TD-B3LYP nor TD-PBE0 provides useful data. Both functionals overestimate the wavelength for the first electronic transition already for **1f** and **2a**, and with the stronger donor rings in **1i** and **2b**, this overestimation becomes dramatic. For **2b** with TD-B3LYP, for example, λ_{max} is calculated about 280 nm too long. This reflects a serious underestimation in the energy required for the charge-transfer interaction in these compounds, which has been documented before in the calculation of other long-range charge-transfer transitions with TD-DFT.[48] Figure 4c shows an overlay of the calculated spectra for **2b**, where the experimental value for the longest-wavelength transition is reported at 508 nm.[52] Interestingly, TD-BH&H produces a λ_{max} of approximately 500 nm, and this good agreement with experiment is true across the series. In fact, the deviation from the experimental value for **1** is about 40 nm; for **1f**, **2**, and **2a**, about 20 nm; for **2b**, even less. This suggests that, for **1i**, the 495 nm value (see footnote [b] to Table 4) should be considered instead of the 377 nm listed, as the larger value again deviates from the experi-

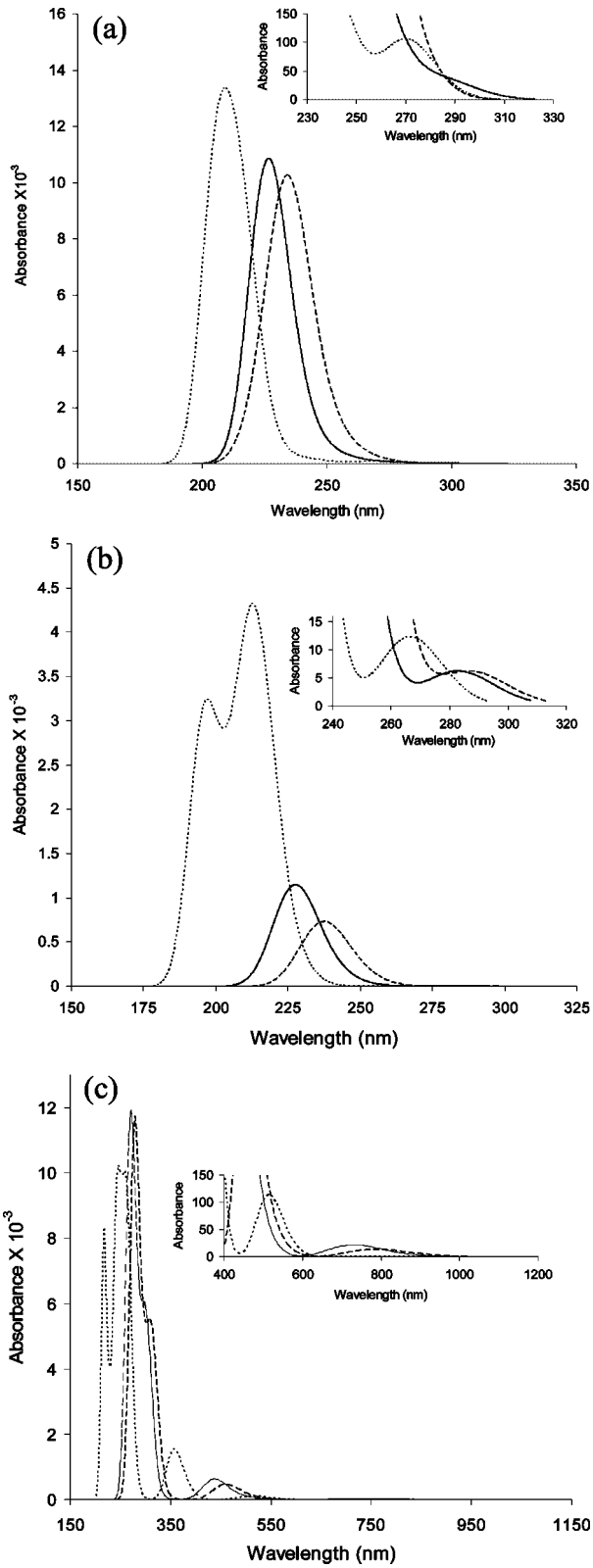

Figure 4. Overlay of simulated [6-31+G(d,p) basis set] UV−vis spectra of (a) **1**, (b) **2** (boat conformer), and (c) **2b** (chair conformer). (− − −) TD-B3LYP, (—) TD-PBE0, and (• • •) TD-BH&H.

mental value by about 20 nm. If one allows for this, the reproduction of the bathochromic (red) shifts from **1f** and **2a** upon introduction of the stronger electron-donating rings in **1i** and **2b** is excellent. For experimental red shifts of 125 and 92 nm in the [2.2] and [3.3] series, respectively, we calculate shifts of 121 and 111 nm with TD-BH&H for the boat conformers.

TABLE 4: Experimental and Calculated [6-31+G(d,p) Basis Set] Wavelengths (nm) and Oscillator Strengths (in Parentheses) for the First Electronic Transitions of 1, 1f, 1i, 2, 2a, and 2b

	exptl	TD-B3LYP	TD-PBE0	TD-BH&H
1	302[a]	271[b] (0.0009)	286 (0.0005)	271 (0.0017)
1f	395sh[c,d]	419[b] (0.0039)	457 (0.0001)	374 (0.0024)
1i	520[c]	752 (0.0001)	703 (0.0001)	377[b] (0.0041)
2 chair	294[a]	243[b] (0.0073)	237[b] (0.0073)	226[b] (0.0078)
2 boat		287 (0.0001)	283 (0.0001)	267 (0.0002)
2a chair	416[c]	502 (0.0057)	478 (0.0072)	391 (0.0158)
2a boat		496 (0.0093)	472 (0.0127)	384 (0.0271)
2b chair	508[b]	787 (0.0002)	730 (0.0003)	515 (0.0016)
2b boat		786 (0.0012)	728 (0.0030)	495 (0.0179)

[a] From ref 24. [b] Longer-wavelength zero-intensity transitions: with B3LYP, 291 nm for **1**, 479 nm for **1f**, 290 nm for **2** chair; with PBE0, 286, 270, and 245 nm for **2** chair; with BH&H, 264 and 245 nm for **2** chair, 495 nm for **1i**. [c] From ref 52. [d] Shoulder.

BH&H has been reported to be capable of reproducing the potential energy surfaces of stacked benzene rings and nucleic acid bases, as well as the lowest-energy conformations of many stacked aromatic compounds.[39] In light of this, the TD-BH&H performance for electronic excitations here is certainly impressive, but maybe not completely unexpected. However, it should be noted that the long-wavelength transitions for compounds **1f**, **1i**, **2a**, and **2b** reflect charge-transfer interactions that are much stronger than those encountered in stacked nucleic acid base pairs, which have λ_{max} values closer to those exhibited by **1** and **2**. Table 4 shows, as was discussed above, that both TD-B3LYP and TD-PBE0 are capable of reproducing the wavelength of the first electronic transition for these systems.

4. Conclusions

We speculated that a potential way of circumventing the problem that DFT functionals have with π-stacking interactions was to introduce a tether between the stacked aromatic rings. From this study on [*n.n*]paracyclophanes, we were able to effectively examine the effects of constraining two interacting aromatic rings on the performance of (TD-)B3LYP, (TD-)PBE0, and (TD-)BH&H for geometries, ionization potentials, and excitation energies. The addition of the tether between the interacting rings improves the performance of PBE0, as is evident from the adequate reproduction of geometries and IPs, whereas B3LYP appears to benefit less. Both TD-B3LYP and TD-PBE0 tend to underestimate charge-transfer excitation energies, giving rise to λ_{max} values in the low-energy region that are grossly exaggerated, whereas for [*n.n*]paracyclophanes with weaker donor−acceptor interactions, experimental wavelengths are reproduced well. In fact, it is the performance on these latter [*n.n*]paracyclophanes that is important, as they have lowest-energy transitions close to those of stacked nucleic acid base pairs (260−280 nm). Although, overall, (TD-)BH&H shows a very good performance in this study, it has been reported to overestimate hydrogen-bond strengths. Therefore, for the description of oligonucleotide fragments, we recommend the use of (TD-)PBE0, as it not only performs just as well as (TD-)BH&H in most contexts here, but is also known to accurately capture the strength of hydrogen bonds.

Acknowledgment. Calculations were performed at the Centre for Research in Molecular Modeling (CERMM), which was established with the financial support of the Concordia University Faculty of Arts and Science, the Ministère de l'Éducation du Québec (MEQ), and the Canada Foundation for Innovation

(CFI). This work was supported by a research grant from the Natural Sciences and Engineering Research Council of Canada (NSERC).

Supporting Information Available: Tables for total energies and zero-point vibrational energies, geometrical parameters, ionization potentials and orbital energies, and figure for basis set dependence of ionization potentials. This material is available free of charge via the Internet at http://pubs.acs.org.

References and Notes

(1) Caramori, G. F.; Galembeck, S. E. *J. Phys. Chem. A* **2007**, *111*, 1705.
(2) Caramori, G. F.; Galembeck, S. E.; Laali, K. K. *J. Org. Chem.* **2005**, *70*, 3242.
(3) Grimme, S. *Chem. Eur. J.* **2004**, *10*, 3423.
(4) Grimme, S.; Antony, J.; Schwabe, T.; Mück-Lichtenfeld, C. *Org. Biomol. Chem.* **2007**, *5*, 741.
(5) Habel, M.; Niederalt, C.; Grimme, S.; Nieger, M.; Vögtle, F. *Eur. J. Org. Chem.* **1998**, *1998*, 1471.
(6) Henseler, D.; Hohlneicher, G. *J. Phys. Chem. A* **1998**, *102*, 10828.
(7) Salcedo, R.; Mireles, N.; Sansores, L. E. *J. Theor. Comput. Chem.* **2003**, *2*, 171.
(8) Walden, S. E.; Glatzhofer, D. T. *J. Phys. Chem. A* **1997**, *101*, 8233.
(9) Černý, J.; Hobza, P. *Phys. Chem. Chem. Phys.* **2005**, *7*, 1624.
(10) González Moa, M. J.; Mandado, M.; Mosquera, R. A. *J. Phys. Chem. A* **2007**, *111*, 1998.
(11) Grimme, S.; Antony, J. *Phys. Chem. Chem. Phys.* **2006**, *8*, 5287.
(12) Hobza, P.; Šponer, J.; Reschel, T. *J. Comput. Chem.* **1995**, *16*, 1315.
(13) Šponer, J.; Leszczyński, J.; Hobza, P. *J. Phys. Chem.* **1996**, *100*, 5590.
(14) Dàbkowska, I.; Gonzalez, H. V.; Jurečka, P.; Hobza, P. *J. Phys. Chem. A* **2005**, *109*, 1131.
(15) Hill, J. G.; Platts, J. A. *J. Chem. Theor. Comput.* **2007**, *3*, 80.
(16) Hobza, P.; Šponer, J. *Chem. Rev.* **1999**, *99*, 3247.
(17) Šponer, J.; Riley, K. E.; Hobza, P. *Phys. Chem. Chem. Phys.* **2008**, *10*, 2595.
(18) Grimme, S. Calculation of the electronic spectra of large molecules In *Reviews of Computational Chemistry*; Lipkowitz, B. K., Larter, R. , Cundari, R. T. , Eds.; John Wiley and Sons: New York, 2004; Vol. 20, p 153.
(19) Lin, I.-C.; Rothlisberger, U. *Phys. Chem. Chem. Phys.* **2008**, *10*, 2730.
(20) Goll, E.; Leininger, T.; Manby, F. R.; Mitrushchenkov, A.; Werner, H.-J.; Stoll, H. *Phys. Chem. Chem. Phys.* **2008**, *10*, 3353.
(21) Brown, C. J.; Farthing, A. C. *Nature* **1949**, *164*, 915.
(22) Lyssenko, K. A.; Antipin, M. Y.; Antonov, D. Y. *Chem. Phys. Chem.* **2003**, *4*, 817.
(23) Hope, H.; Bernstein, J.; Trueblood, K. N. *Acta Crystallogr. B* **1972**, *28*, 1733.
(24) Cram, D. J.; Allinger, N. L.; Steinberg, H. *J. Am. Chem. Soc.* **1954**, *76*, 6132.
(25) Frontera, A.; Quiñonero, D.; Garau, C.; Costa, A.; Ballester, P.; Deyà, P. M. *J. Phys. Chem. A* **2006**, *110*, 5144.
(26) Bräse, S.; Dahmen, S.; Höfener, S.; Lauterwasser, F.; Kreis, M.; Ziegert, R. E. *Syn. Lett.* **2004**, 2647.
(27) Dyson, P. J.; Humphrey, D. G.; McGrady, J. E.; Mingos, M. P.; Wilson, D. J. *J. Chem. Soc., Dalton Trans.* **1995**, 4039.
(28) Albrecht, M. *Chem. Soc. Rev.* **1998**, *27*, 281.
(29) Shibahara, M.; Watanabe, M.; Iwanaga, T.; Matsumoto, T.; Ideta, K.; Shinmyozu, T. *J. Org. Chem.* **2008**, *73*, 4433.
(30) Frisch, M. J.; Trucks, G. W.; Schlegel, H. B.; Scuseria, G. E.; Robb, M. A.; Cheeseman, J. R.; Montgomery, J. A., Jr.; Vreven, T.; Kudin, K. N.; Burant, J. C.; Millam, J. M.; Iyengar, S. S.; Tomasi, J.; Barone, V.; Mennucci, B.; Cossi, M.; Scalmani, G.; Rega, N.; Petersson, G. A.; Nakatsuji, H.; Hada, M.; Ehara, M.; Toyota, K.; Fukuda, R.; Hasegawa, J.; Ishida, M.; Nakajima, T.; Honda, Y.; Kitao, O.; Nakai, H.; Klene, M.; Li, X.; Knox, J. E.; Hratchian, H. P.; Cross, J. B.; Bakken, V.; Adamo, C.; Jaramillo, J.; Gomperts, R.; Stratmann, R. E.; Yazyev, O.; Austin, A. J.; Cammi, R.; Pomelli, C.; Ochterski, J. W.; Ayala, P. Y.; Morokuma, K.; Voth, G. A.; Salvador, P.; Dannenberg, J. J.; Zakrzewski, V. G.; Dapprich, S.; Daniels, A. D.; Strain, M. C.; Farkas, O.; Malick, D. K.; Rabuck, A. D.; Raghavachari, K.; Foresman, J. B.; Ortiz, J. V.; Cui, Q.; Baboul, A. G.; Clifford, S.; Cioslowski, J.; Stefanov, B. B.; Liu, G.; Liashenko, A.; Piskorz, P.; Komaromi, I.; Martin, R. L.; Fox, D. J.; Keith, T.; Al-Laham, M. A.; Peng, C. Y.; Nanayakkara, A.; Challacombe, M.; Gill, P. M. W.; Johnson, B.; Chen, W.; Wong, M. W.; Gonzalez, C.; Pople, J. A. *Gaussian 03*, revision C.02; Gaussian, Inc.: Pittsburgh, PA, 2004.
(31) Jenson, F. *Introduction to Computational Chemistry*, 2nd ed.; John Wiley & Sons Ltd.: West Sussex, U.K., 2007.
(32) Becke, A. D. *J. Chem. Phys.* **1993**, *98*, 1372.
(33) Lee, C.; Yang, W.; Parr, R. G. *Phys. Rev. B.* **1988**, *37*, 785.
(34) Stephens, P. J.; Devlin, F. J.; Chabalowski, C. F.; Frisch, M. J. *J. Phys. Chem.* **1994**, *98*, 11623.
(35) (a) Perdew, J. P.; Burke, K.; Ernzerhof, M. *Phys. Rev. Lett.* **1996**, *77*, 3865. (b) Perdew, J. P.; Ernzerhof, M.; Burke, K. *J. Chem. Phys.* **1996**, *105*, 9982. (c) Perdew, J. P.; Burke, K.; Ernzerhof, M. *Phys. Rev. Lett.* **1997**, *78*, 1396.
(36) Hobza, P.; Šponer, J. *Chem. Rev.* **1999**, *99*, 3247.
(37) Jurečka, P.; Hobza, P. *J. Am. Chem. Soc.* **2003**, *125*, 15608.
(38) Santoro, F.; Barone, V.; Improta, R. *J. Comput. Chem.* **2008**, *29*, 957.
(39) Waller, M. P.; Robertazzi, A.; Platts, J. A.; Hibbs, D. E.; Williams, P. A. *J. Comput. Chem.* **2006**, *27*, 491.
(40) Møller, C.; Plesset, M. S. *Phys. Rev.* **1934**, *46*, 618.
(41) Tsuzuki, S.; Honda, K.; Uchimaru, T.; Mikami, M. *J. Chem. Phys.* **2004**, *120*, 647.
(42) Petersson, G. A.; Bennett, A.; Tensfeldt, T. G.; Al-Laham, M. A.; Shirley, W. A.; Mantzaris, J. *J. Chem. Phys.* **1988**, *89*, 2193.
(43) Koopmans, T. *Physica* **1934**, *1*, 104.
(44) Muchall, H. M.; Werstiuk, N. H. *Can. J. Chem.* **2006**, *84*, 1124.
(45) Zhang, L.; Peslherbe, G. H.; Muchall, H. M. *Photochem. Photobiol.* **2006**, *82*, 324.
(46) Bhattacharya, S. *Chem. Phys. Lett.* **2007**, *446*, 199.
(47) Dreuw, A.; Weisman, J. L.; Head-Gordon, M. *J. Chem. Phys.* **2003**, *119*, 2943.
(48) Dreuw, A.; Head-Gordon, M. *Chem. Rev.* **2005**, *105*, 4009.
(49) Dreuw, A.; Head-Gordon, M. *J. Am. Chem. Soc.* **2004**, *126*, 4007.
(50) Gorelsky, S. I. *SWizard program*, revision 4.4; CCRI, University of Ottawa: Ottawa, Canada, 2008; see http://www.sg-chem.net/ (last accessed Aug 2008).
(51) (a) Portmann, S.; Lüthi, H. P. *Chimia* **2000**, *54*, 766. (b) Flükiger, P.; Lüthi, H. P.; Portmann, S.; Weber, J. Molekel 4.3; Swiss National Supercomputing Centre (CSCS): Manno, Switzerland, 2002.
(52) Staab, H. A.; Krieger, C.; Wahl, P.; Kay, K.-Y. *Chem. Ber.* **1987**, *120*, 551.
(53) Furo, T.; Mori, T.; Wada, T.; Inoue, Y. *J. Am. Chem. Soc.* **2005**, *127*, 8242.
(54) Almenningen, A.; Bastiansen, O. *J. Mol. Struct.* **1985**, *128*, 59.
(55) Bastiansen, O.; Samdal, S. *J. Mol. Struct.* **1985**, *128*, 115.
(56) Charbonneau, G.-P.; Delugeard, Y. *Acta Crystallogr. B* **1976**, *B32*, 1420.
(57) Gerzain, M.; Buchanan, G. W.; Driega, A. B.; Facey, G. A.; Enright, G.; Kirby, R. A. *J. Chem. Soc., Perkin Trans. 2* **1996**, 2687.
(58) Gantzel, P. K.; Trueblood, K. N. *Acta Crystallogr.* **1965**, *18*, 958.
(59) Anet, F. A. L.; Brown, M. A. *J. Am. Chem. Soc.* **1969**, *91*, 2389.
(60) Boschke, F. L. *Cyclophanes II*; Topics in Current Chemistry Series; Springer: Berlin, 1983; Vol. 115.
(61) Muchall, H. M. Ultraviolet Photoelectron Spectra of Cyclophanes. In *Modern Cyclophane Chemistry*; Gleiter, R., Hopf, H. , Eds.; Wiley-VCH: Weinheim, Germany, 2004; p 259.
(62) Blackburn, G. M.; Gait, M. J. *Nucleic Acids in Chemistry and Biology*, 2nd ed.; Oxford University Press: Oxford, U.K., 1996.

JP808144E